Transitional and Turbulent Heat-Transfer Measurements on a Yawed Blunt Conical Nosetip

GEORGE F. WIDHOPF*
The Aerospace Corporation, Los Angeles, Calif.
AND
ROBERT HALL†
U.S. Naval Ordnance Laboratory, Silver Spring, Md.

Transitional and turbulent heat-transfer rates measured on a blunt ($R_N = 2.5$ in.) nine degree half-angle cone in a $M_\infty = 5$ air flow at various angles of attack are presented. Measurements were made at nominal freestream Reynolds numbers of 48.5, 19, and $11(10)^6$/ft and nominal angles of attack of $\alpha = 0°$, 5°, 10°, 15°, 20°, and 27°. The wall to stagnation temperature ratio varied between 0.20 and 0.29. Detailed circumferential ($\Delta\phi \approx 30°$) and axial ($S/R_N \leq 5.25$) distributions of both the heat-transfer rate and surface pressure were obtained over the entire model at each test condition and angle of attack. Natural transition occurred on the hemisphereical cap near the stagnation region at the $Re_\infty = 48.5$ and $19(10)^6$ test conditions. Heat-transfer rates computed along inviscid surface streamlines using various simplified heat-transfer formulations are compared to the data. The Vaglio-Laurin type turbulent heat-transfer formulations are shown to be in good agreement with the data at all test conditions, while those formulations which use reference rather than edge conditions to define the local rate, substantially overpredict the heat-transfer rate over the entire surface. The applicability of the angle-of-attack turbulent heat-transfer correlation previously proposed by Widhopf is demonstrated for the present test results.

Nomenclature

A = defined by Eq. (5a)
h = heat transfer coefficient $= q_w/(T_r - T_w)$, static enthalpy
h_2 = length element which characterizes the spreading of the streamlines
H = total enthalpy
H_r = recovery enthalpy
l = length element along a streamline measured from the most forward point on the surface
M = Mach number
p = static pressure
$\bar{P}$ = nondimensionalized pressure, p/p_0
P_r = Prandtl number (a value of 0.716 was used exclusively)
q = heat transfer per unit area per unit time
q_{cw} = cold wall heat-transfer rate
Re = Reynolds number per foot
R_N = nose radius
S = surface coordinate
T = temperature
U = velocity
α = angle of attack
δ = wall thickness
ε = defined by Eq. (5a)
μ = coefficient of viscosity
ν = kinematic viscosity, μ/ρ
ρ = density
ϕ = circumferential angle measured from leeward ray

Subscripts

e = boundary-layer edge conditions
se = boundary-layer edge stagnation conditions
T = transition point
w = wall conditions
0 = laminar stagnation point condition
1, 3, 4 = reference conditions used in Eqs. (2, 3, and 4) respectively, which are defined using Eq. (5b)
∞ = freestream conditions

Presented as Paper 72–212 at the AIAA 10th Aerospace Sciences Meeting, San Diego, Calif., January 17–19, 1972; submitted January 17, 1972; revision received June 8, 1972. The authors wish to acknowledge the assistance of M. E. Falusi (NOL) in the reduction of the wind-tunnel data and the assistance of R. Harriman (Aerospace Corporation) in the organization and plotting of the final data. Thanks are also extended to K. Reed (Aerospace Corporation) for his efficient coding and running of streamline tracing program and to F. Fernandez (Aerospace Corporation) who originally suggested this work.

Index category: Boundary Layers and Convective Heat Transfer—Turbulent.

* Member of the Technical Staff. Associate Member AIAA.
† Aerospace Engineer.

Introduction

VERIFICATION of the accuracy of any proposed numerical method of calculating the heat-transfer rate to the surface of a hypersonic re-entry vehicle invariably depends upon its subsequent agreement with experimental data. This becomes even more pertinent when three-dimensional transitional and turbulent flows are considered. At present, there is a need for angle-of-attack heat-transfer data wherein the flow undergoes a natural transition from the laminar to the turbulent state on the blunt portion of the nosetip at a location close to the stagnation region. It is especially desirable to achieve the fully turbulent state near the sonic point so that measurements of the peak heating can be obtained. In this regard, detailed measurements over the entire region encompassing the first few nose radii are needed. Also, since most re-entry conditions are characterized by low wall-to-stagnation temperature ratios, the test conditions should also adequately simulate this parameter. The simulation of these conditions will then provide a good experimental data base which can then be used to determine the accuracy of the various proposed numerical methods.

Previous investigations have not adequately simulated all of these conditions. In Ref. 1 an extensive investigation of the fully turbulent heat-transfer rate on the conical surface of a blunt cone at various angles of attack was presented. Unfortunately, in that study the spherical cap had to be roughened in order to sustain the turbulent flow and prevent the flow from relaminarizing. Thus, the heat-transfer rates on the hemisphere could not be obtained. Included in Ref. 2 is a study of the leeward plane heat-transfer distribution at angle of attack.

This paper presents the results of a test program wherein the previously outlined conditions were simulated. Heat-transfer and static pressure distributions over a blunt cone at various angles-of-attack are presented at three different freestream conditions. The results of some numerical calculations of the turbulent heat-transfer rate, utilizing various (five) methods proposed in the literature, are compared to the data and the applicability of an angle-of-attack turbulent heat-transfer correlation[3] previously proposed by one of the authors is also investigated.

Experimental Facility and Test Conditions

The test program was conducted in the U.S. Naval Ordnance Laboratory Hypersonic Tunnel 8 Facility.[4,5] The measurements were made in an air environment at a freestream Mach number of 5 and at nominal freestream Reynolds numbers of 48.5, 19 and 11(10)^6/ft. The model was cooled with liquid nitrogen and the resulting wall to stagnation temperature ratio obtained using this procedure varied between $0.20 \leqq T_w/T_o \leqq 0.29$. The nominal angles-of-attack considered included $\alpha = 0°$, 5°, 10°, 15°, 20° and 27.5°.

Model Configuration and Instrumentation

The configuration utilized was a spherically capped (R_N = 2.5 in.) 9° half-angle cone. Two models were fabricated for use in this test program. A thick wall (δ = 0.187 in.) model was constructed of brass and used during the pressure measurement phase of the program. The heat-transfer model consisted of a thin wall shell (δ = 0.025 in.) fabricated of ARMCO 17-4PH stainless steel. After fabrication, the surface was heat treated to condition H-1150 and polished to an 8 μ finish. Webs were used for internal support and were positioned so that they would not interfere with or influence the measurements.[6] Both the surface pressure (95 gages) and heat transfer (73 gages) were measured at each freestream condition previously described, at approximately eleven axial stations (S/R_N = 0.15, 0.30, 0.45, 0.60, 0.75, 0.90, 1.05, 1.30, 1.50, 2.0, 3.5, 5.25), along seven circumferential rays (φ = 0°, 40°, 70°, 90°, 120°, 150°, and 180°). The detailed location of both types of instrumentation is given in Ref. 6.

The heat-transfer measurements were made utilizing 0.005 in. diam chromel-alumel thermocouples, whose response were automatically recorded by the NOL high-speed data acquisition system.[7] The resulting data were then reduced using the calorimeter technique described in Ref. 8, and corrected for initial transient conduction errors using the method of Ref. 9. A detailed description of the data reduction technique is included in Refs. 6 and 10. Possible sources of error were examined and are discussed in these references. The heat-transfer coefficient h was directly determined from the thermocouple output and subsequently corrected for initial transient conduction errors. The data presented herein, is in terms of the cold wall heat-transfer rate q_{cw} defined as $q_{cw} = hT_{se}$.

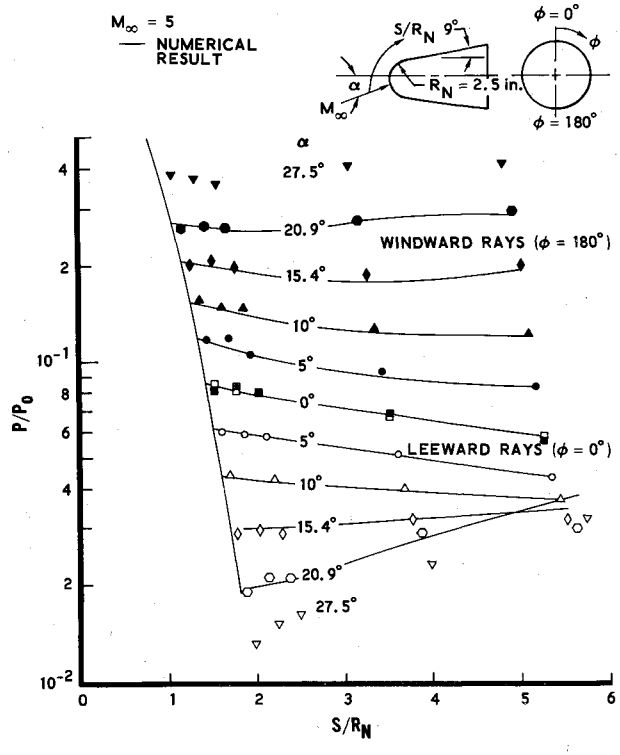

Fig. 1 Surface pressure distributions along the windward and leeward rays for various angles of attack.

The pressure measurements were made utilizing surface pressure taps connected to strain-gage pressure tranducers[11] housed in two sealed water-cooled containers mounted in the test cell.

The accuracy of the heat-transfer measurements is estimated to be $\pm 10\%$ for most of the range of the measurements, whereas the accuracy is approximately $\pm 15\%$ near regions of somewhat discontinuous slope in heat transfer distribution (i.e., transition region and sphere-cone junction) and near the stagnation region at the higher angles-of-attack. The accuracy of the pressure measurements is approximately $\pm 5\%$.

Experimental Results

Only representative data plots which depict the pertinent results determined in this study are included in this paper. Tabulations of the data at each of the individual test conditions are included in Ref. 6. Initially, an overview of the data will be given and then comparisons with various numerical calculations will be presented and discussed in the next section.

Shown in Fig. 1 are the windward and leeward pressure distributions on the conical surface for the angles-of-attack considered in this test program. Included in this figure are the numerical results obtained using the angle-of-attack inviscid flowfield computer code described in Ref. 12. Good agreement between the numerical calculations and the measured distributions is noticed (except in regions where viscous-inviscid interactions should be important) for all angles of attack at which the calculations could be made.

Included in Figs. 2 are the corresponding plots of the heat-transfer distributions on the conical surface for the three different freestream conditions at which tests were conducted. It should be noted that the distributions of both the heat transfer and the pressure are similar. Also, as the angle of attack is increased, it is seen that the heat transfer on the leeward side decreases at a faster rate than it increases on the windward ray. It should be pointed out that the flow is transitional[6] along the windward ray for α = 20.25° and 27.5° at the Re_∞ = 11(10)^6 freestream condition.

Shown in Fig. 3a is the nondimensional cold wall heat-transfer (q_{cw}/q_{cw_0}) distribution on the hemispherical cap plotted with respect to the nondimensional streamline coordinate l/R_N. (All values of q_{cw_0} appearing in the paper are calculated values obtained using the Fay and Riddell[13] relationship). Here the data for each of the angles-of-attack considered at the Re_∞ = 48.5(10)^6 condition have been superimposed on one figure. This type of plot is convenient, since the angle-of-attack distributions on the hemisphere should be self-similar in this coordinate system. Indeed, within the stated experimental error, this is the case. At this freestream condition, the flow becomes transitional at approximately station l/R_N = 0.2 and achieves the fully turbulent state at approximately l/R_N = 0.4, thus, the peak heating point has been measured. The T_w/T_o ratio varied between 0.24 to 0.27 for these tests and to a small degree some of the broadening of the transition region[14] can be attributed to this variation. Similar plots for individual tests at Re_∞'s of 19(10)^6 and 11(10)^6 are shown in Figs. 3b and 3c. In these figures, each of the individual circumferential data points have been indicated and the transition from the laminar to the turbulent state is clearly shown. It is also interesting to note (Figs. 2–3) that the peak heating point is still on the hemisphere for angles of attack up to three times the cone half angle.

The location of the transition point at each of these freestream conditions was determined by plotting the heat-transfer distributions on a log-log scale and determining the intersection of two straight lines drawn through the laminar and transitional data.[15] The transition points were also determined by matching the distributions with a numerically calculated heat-transfer distribution of the type discussed in the next section. Each of

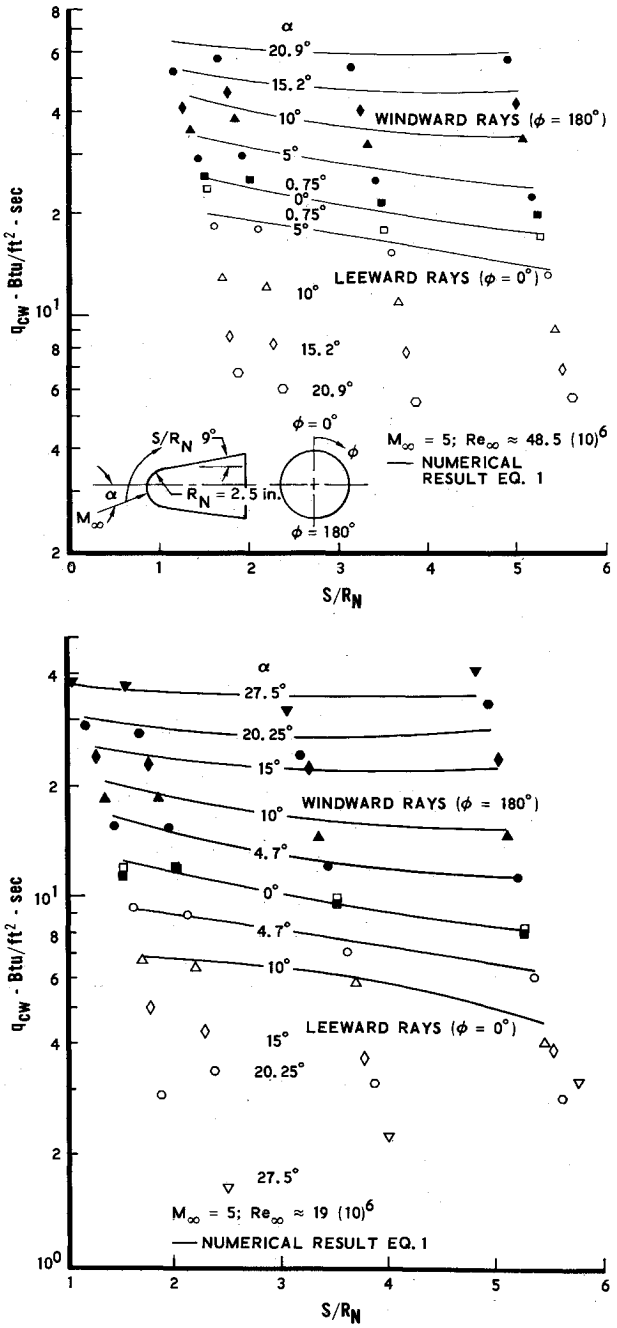

these methods is subject to error,[6] but are accurate enough to allow for a relatively accurate determination of the transition point.

The results obtained for a few runs at the $Re_\infty = 48.5$ and $19(10)^6$ conditions are shown in Fig. 4. The results obtained by the two methods discussed previously are indicated by the designations Method 1 and 2, respectively. Included in this figure are various transition data obtained on smooth blunt nosetips, which were originally compiled in Ref. 16. Here the value of Re_Θ at the transition point has been plotted against the corresponding edge Mach number, M_{e_T}. Each of the test conditions are indicated in the legend of the figure and the variation in the T_w/T_o ratio should be noticed. These present variables (Re_{Θ_T} and M_{e_T}) certainly cannot adequately represent the variation of the transition location with all the pertinent variables which effect the transition process, but it is evident from this figure that natural transition was achieved at these two test conditions. Similar results obtained for the $Re_\infty = 11(10)^6$ condition, indicate that the boundary-layer was prematurely tripped by some surface roughness which probably resulted from particle impacts. This occurred even though the model was hand polished between runs.

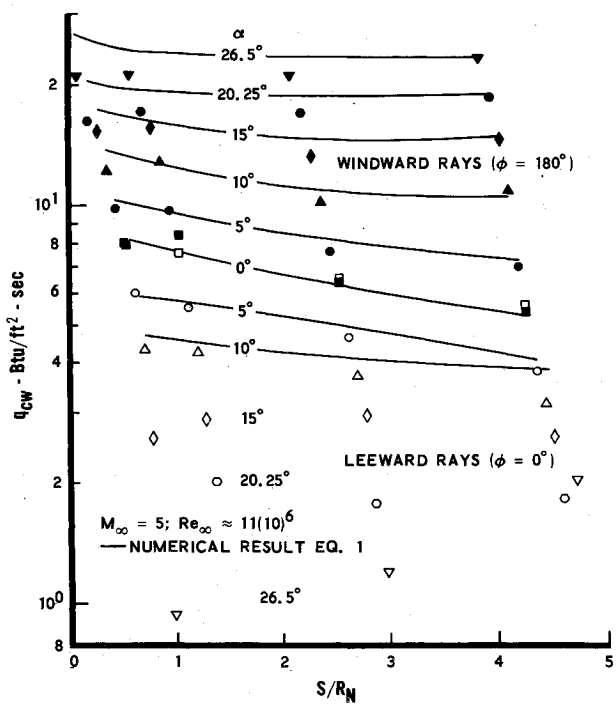

Figs. 2 Heat-transfer distributions along the windward and leeward rays for various angles of attack.

When the heat-transfer ratio along any ray (or rather for any specific point on the surface) was plotted on a semilog scale as a function of angle of attack, the variation was found to be approximated very well by a straight line. This was the case as long as the flow was fully turbulent and not separated. An example of this is shown in Fig. 5 for specific locations on the windward and leeward rays at the $Re_\infty = 48.5(10)^6$ freestream condition. Analagous examples for the other freestream conditions are included in Ref. 6. This behavior was also observed in Ref. 1 and simplifies interpolations of the data to any inclusive angle of attack. As was found in Ref. 1, the yaw plane heat-transfer rate on the conical surface is a very weak function of angle-of-attack. An example of this can be seen in Fig. 6 where the variation of the circumferential turbulent heat-transfer distribution with angle of attack, at station $S/R_N = 5.25$, is shown for the $Re_\infty = 48.5(10)^6$ freestream condition.

The variation of the circumferential heat-transfer distribution for various axial surface location, measured with respect to the model centerline, is shown in Fig. 7. This type of planar section is interesting since it shows the circumferential variation in the geometric plane. In general, once the flow has become fully turbulent, the circumferential variation can be described by a cosine type variation. However, the distributions in the transitional regime become varied indeed, since at angle-of-attack, the windward transition point moves rearward, with respect to a coordinate system centered at the $\alpha = 0°$ stagnation point, while the leeward transition point moves forward. The subsequent effect of this type of heating distribution on nosetip ablation and the resulting shape change can be visualized.

Comparison with Numerical Results

Heat-transfer rates computed along inviscid surface streamlines traced[1,6] over the surface of the blunt cone at each angle of attack were compared to the data. The Fay and Riddell relation[13] was used to calculate the stagnation heat flux and Vaglio-Laurin's laminar relation[17] was used to obtain the laminar heat-transfer distribution. Four separate formulations were used to calculate the fully turbulent heat-transfer rate, whereas the method of Ref. 18 was applied to the angle-of-attack case and used to determine the distribution in the transi-

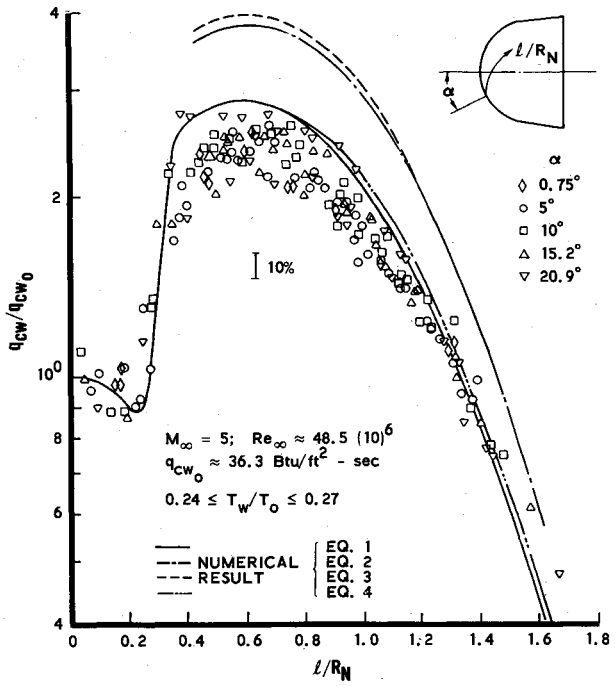

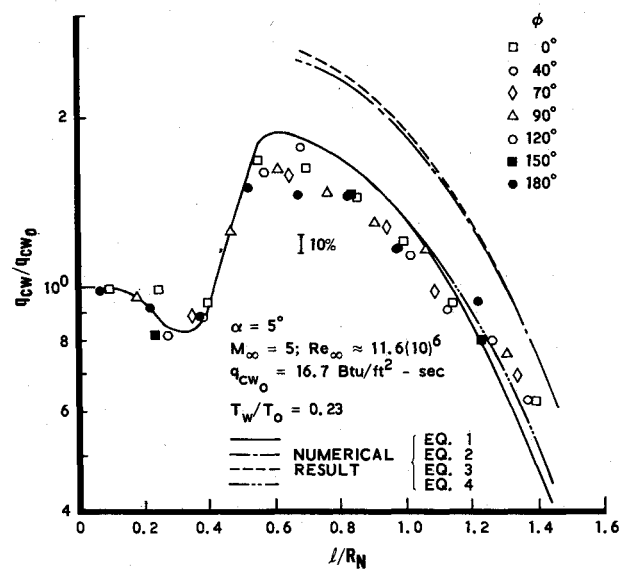

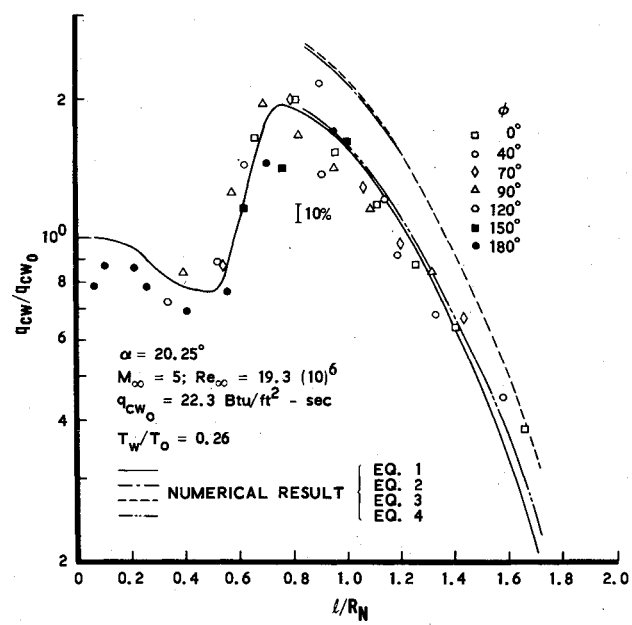

Figs. 3a-c Heat-transfer distribution on the hemispherical cap.

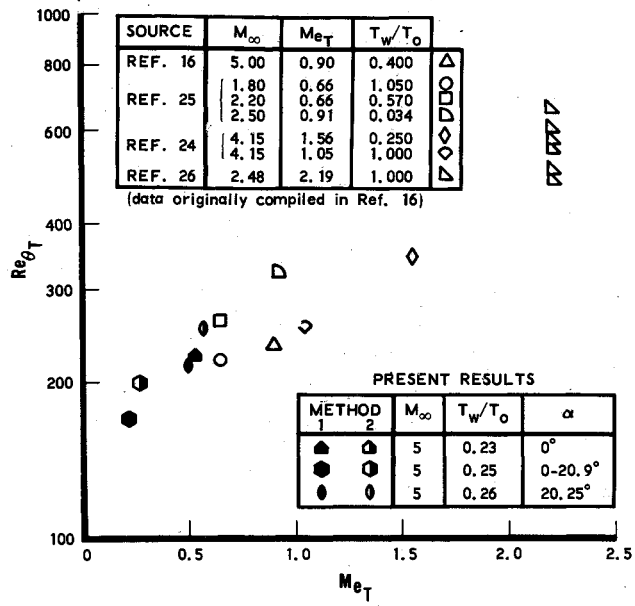

Fig. 4 Smooth wall transition data on blunt nosetips.

tional regime. The four methods are those proposed by Vaglio-Laurin,[19] McCuen et al.,[20] Walker,[21] and DeJarnette and Tai.[22] These formulations are given below, in their respective order

$$q_w = A(H_{se} - H_w)\rho_e U_e h_2^{1/4} \mu_e \mu_{se}^{-3/5} \left\{ \int_o^l \rho_e U_e \mu_e h_2^{5/4} dl \right\}^{-1/5} \tag{1}$$

$$q_w = A(H_r - H_w)^{5/4} \rho_1 U_2 (h_2 \mu_1)^{1/4} \left\{ \int_o^l \rho_1 U_e \mu_1^{1/4} [h_2(H_r - H_w)]^{5/4} dl \right\}^{-1/5} \tag{2}$$

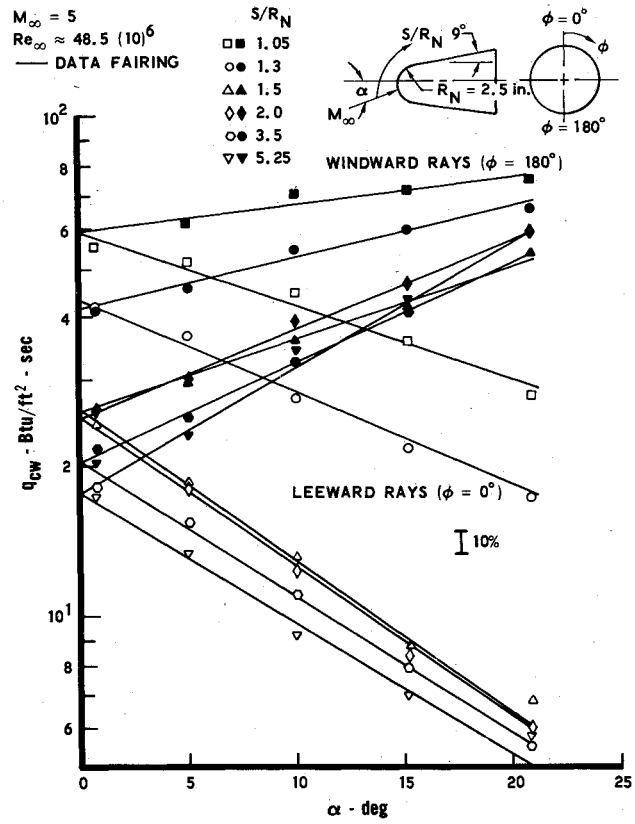

Fig. 5 Heat-transfer variation with angle of attack at various stations along the windward and leeward rays.

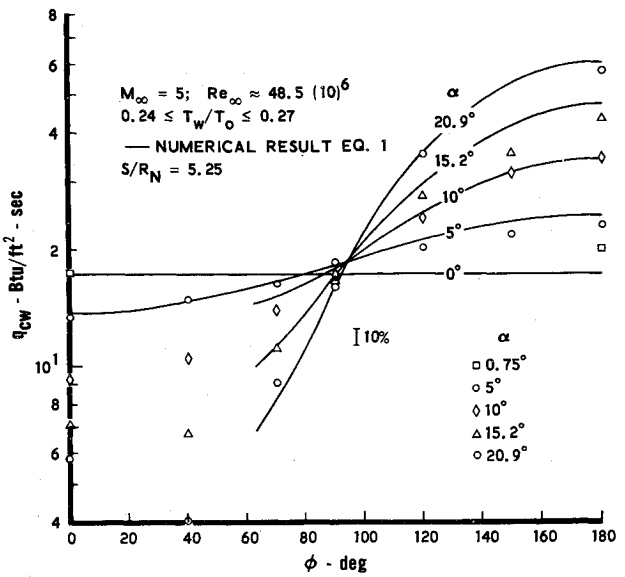

Fig. 6 Comparison between experimental and calculated circumferential turbulent heat-transfer distributions at station $S/R_N = 5.25$ for various angles of attack.

$$q_w = A[(H_r - H_w)\varepsilon]^{5/4}\rho_e U_e(\mu_e h_2)^{1/4} \left\{\int_o^l \rho_e U_e \mu_e^{1/4}[(H_r - H_w)h_2\varepsilon]^{5/4}dl\right\}^{-1/5} \quad (3)$$

$$q_w = A(H_{se} - H_w)\rho_e^{1.05}U_e h_2^{1/4}\mu_e^{4/5}\nu_4^{1/20}\mu_{se}^{-3/5} \left\{\int_o^l \rho_e^{5/4}U_e\nu_4^{1/4}h_2^{5/4}dl\right\}^{-1/5} \quad (4)$$

where

$$A = 0.0296\,P_r^{-2/3}$$
$$\varepsilon = (\mu_3/\mu_e)^{1/5}(\rho_3/\rho_e)^{4/5} \quad (5a)$$

and

$$h_1 = 0.36\,h_e + 0.19H_r + 0.45H_w$$
$$h_3 = (0.5 - 0.22\,P_r^{1/3})h_e + 0.22\,P_r^{1/3}H_{se} + 0.5\,H_w \quad (5b)$$
$$h_4 = 0.5\,h_e + 0.5\,H_w + 0.22\,P_r^{1/3}[(\gamma - 1)/2]M_e^2 h_e$$

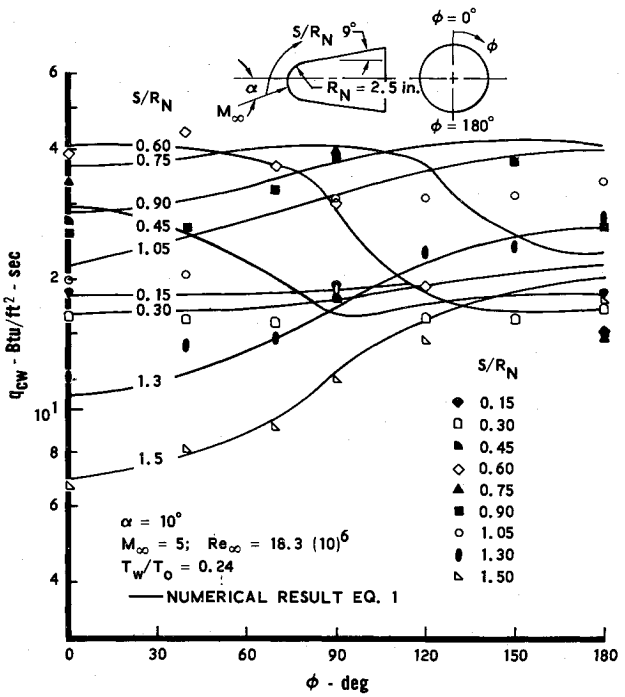

Fig. 7 Circumferential variation of the heat-transfer at various stations on the hemisphere.

Equations 5b define the reference enthalpy which is used together with the pressure to define the reference conditions ρ_1, μ_1, ρ_3, μ_3, and ν_4 used in Eqs. (2–4).

Substitution of Eq. (5a) into Eq. (3) demonstrates that Eqs. (2) and (3) are of exactly the same form, except that the definition of their respective reference conditions [Eqs. (5b)] are slightly different. Similarly, a comparison of Eqs. (1) and (4) will show that Eq. (4) is only slightly different than Eq. (1), being very weakly dependent on reference conditions.

The major difference between the two groups is the use of edge and/or reference conditions to define the local heat-transfer rate. In general, the heat-transfer level predicted by these two groups is different, with the disagreement increasing as the T_w/T_o ratio decreases. In this regard, the data obtained from this test program are especially suited to determine which is the better approximation at moderate cold wall conditions.

The streamline patterns were determined[1,6] using the experimental pressure distributions and were computed from the most forward point on the model to the most rearward station. Thus, the effect of streamline spreading was included in all of these calculations. Perfect gas properties were used and entropy swallowing was neglected. This latter approximation is a good assumption over most of the range of conditions examined herein, except at the higher angles-of-attack on the leeward side.[1] It must be emphasized that the identical freestream conditions, surface pressure distributions, edge conditions, viscosity relation (Sutherland model) and Prandtl number (Pr = 0.716) were used in Eqs. (1–5) in evaluating the heat transfer at a specific test condition. Thus, any variation in the subsequent heat-transfer rate for a given test, is only due to the model itself. Each relation [Eqs. (1–4)] was appropriately modified ($H_{r,se} - H_w \equiv H_{se}$) so the numerical results could be directly compared to the data.

Shown in Figs. 3a–c are the results of some of these comparisons. In general, the results obtained using Eqs. (2–4) are shown downstream of the point where the fully turbulent rate has been achieved. However, for the Vaglio-Laurin formulation [Eq. (1)], the theory of Ref. 18 has been applied to describe the transition from the laminar to the turbulent state. Here it is noticed that the Vaglio-Laurin distribution agrees, within the experimental error, with the data for each of the freestream conditions tested. In all cases, Eq. (4) yielded essentially (always a few percent higher) the same distribution as Eq. (1), thus it was not included where it would degrade the clarity of the respective figure. For each test condition, Eqs. (2) and (3) yield, essentially, the same results for these test conditions except for the effect of the different reference enthalpy formulation near the peak heating point, and thus, only one numerical determined curve in shown in most figures. The distribution in the transitional regime is adequately predicted by the theory of Ref. 18, although more comprehensive statements cannot be made

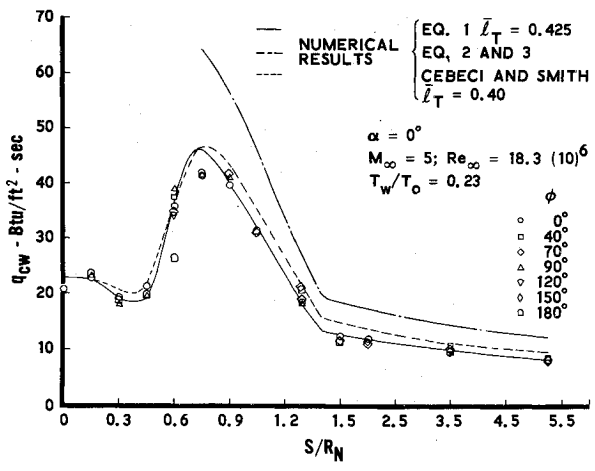

Fig. 8 Comparison between the experimental and numerical heat-transfer distributions at $\alpha = 0°$; $Re_\infty = 18.3(10)^6$.

without a more detailed determination of the heat-transfer distribution in this region.

Figure 8 shows the heat-transfer rate distribution for the zero angle-of-attack case at the $Re_\infty = 19(10)^6$ test condition. It should be pointed out that for this particular case the neglection of entropy swallowing effects is a very good approximation since only the first five nose radii are being considered. Included in this figure is a numerical result‡ obtained using the finite difference turbulent boundary-layer program described in Ref. 23. The identical pressure distribution and edge conditions were used in this calculation, as well. This boundary-layer program uses an eddy viscosity model which accounts for pressure gradient effects. The resulting distribution on the hemisphere falls between the other results, and overpredicts the level on the conical surface. Equation (1) shows good agreement with the data, while Eqs. (2) and (3) substantially overpredict the data over the entire surface. This trend was found to hold for all the measured distributions at each angle of attack. Examples of this trend along the conical surface are shown in Figs. 9a–b, where the longitudinal distribution along various rays are shown for two angles-of-attack, $\alpha = 15°$ and $\alpha = 20.25°$. Here it is noticed that the distributions computed using Eq. (1) show good agreement with the data, while the corresponding rates obtained using Eqs. (2) and (3) do not. Only the $\varphi = 180°$ and 90° solutions, obtained using Eqs. (2) and (3), have been presented in these figures in order to clarify the presentation. Further comparisons between the experimental data and the numerical results obtained using Eq. (1) are shown in Figs. 2a–c for the windward and leeward rays at various angles of attack for each freestream test condition. In general, the agreement is good.

The comparison between the numerical and experimental circumferential heat-transfer distributions on the hemisphere using Eq. (1) and the transitional theory of Ref. 18 is shown in Fig. 7. The agreement in both magnitude and distribution is good, even in the transitional regime. The calculated circumferential distributions at station $S/R_N = 5.25$ were compared to the data for each of the angles of attack, and the results are shown in Fig. 6. The agreement between the numerical results and the measured distributions is good for all the angles of attack, except on the leeward side at the higher angles of attack. In this region, entropy swallowing should become important,[1] thus agreement in this region would not be expected. Also, at the higher angles of attack, separation has occurred on portions of the leeward side, thus the approach used herein is invalid in those regions. An indication of the location of the separation region can be obtained from the circumferential pressure plots included in Ref. 6.

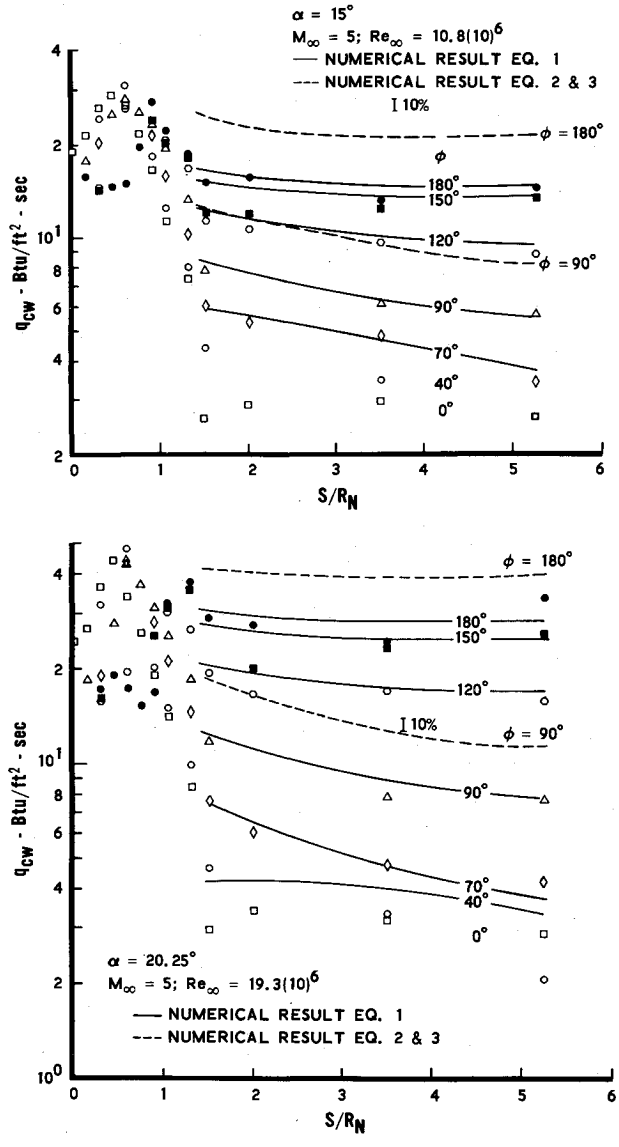

Figs. 9a-b Comparison between the experimental and numerical longitudinal heat-transfer distributions on the conical surface.

Correlations

A simple correlation of the nondimensional turbulent heat-transfer rate (q_w/q_{w_0}) with the nondimensional pressure ratio (p/p_o) for blunt cones at angle of attack was demonstrated in Ref. 3 for a particular set of experimental turbulent heat-transfer measurements.[1] There it was shown that if the nondimensional heat-transfer rate, at a given location on the cone (as measured in a coordinate system whose origin is located at the most forward portion of the body at a given angle of attack), was plotted against the corresponding local nondimensional surface pressure for a spectrum of angles of attack and circumferential locations, it could be correlated at each station by a power law of the form $q_{cw}/q_{cw_0} = A_c\bar{P}^B$. Furthermore, each of the power laws (one for each streamwise surface location) in the set had the same exponent, B. It was also shown that the coefficient A_c of each of these power laws could be accurately determined from the $\alpha = 0°$ heat-transfer distribution, when it was calculated including the effect of entropy swallowing. Thus, given the angle of attack pressure distributions and the $\alpha = 0°$ heat-transfer distribution, the heat-transfer distribution over the entire conical surface (axially as well as circumferentially) could be generated in a simple manner over a spectrum of angles of attack. This evaluation would include three-dimensional as well as entropy swallowing effects. It was also shown that the exponent B was a weak function of the specific heat ratio γ and ω, where $\mu \propto T^\omega$.

Thus, the present experimental results were plotted in this manner in order to determine if the correlation did indeed apply at the present test conditions. The results are shown in Fig. 10 for the $Re_\infty = 48.5(10)^6$ test condition. Here it is seen that the present data can also be correlated by a set of power laws, each having the same exponent (0.96) determined in Ref. 3. The levels of these curves can also be predicted by the $\alpha = 0°$ distribution.[6] Thus, this type of correlation has been shown to be applicable for another set of turbulent heat-transfer data.

Summary and Conclusions

The results of this investigation can be summarized by the following:

1) Smooth wall heat-transfer measurements at low T_w/T_o ratios were obtained at two freestream conditions [$Re_\infty = 48.5$ and $19(10)^6$] over a range of angles of attack. Natural transition

‡ This result was graciously supplied by N. Jaffe of The Aerospace Corp.

was obtained near the stagnation region at both of these test conditions. Premature transition occurred at the $Re_\infty = 11(10)^6$ test condition.

2) Measurements of the peak turbulent heating were obtained on the hemispherical cap at the $Re_\infty = 48.5(10)^6$ test condition. Detailed measurements of the heat-transfer rate were obtained over the entire nosetip at each test condition.

3) Numerical calculations performed using the Vaglio-Laurin turbulent heat-transfer relation are in good agreement with the data. Other formulations which were examined did not agree with the data as well as the results obtained using the Vaglio-Laurin relation. Each of these other relations use reference

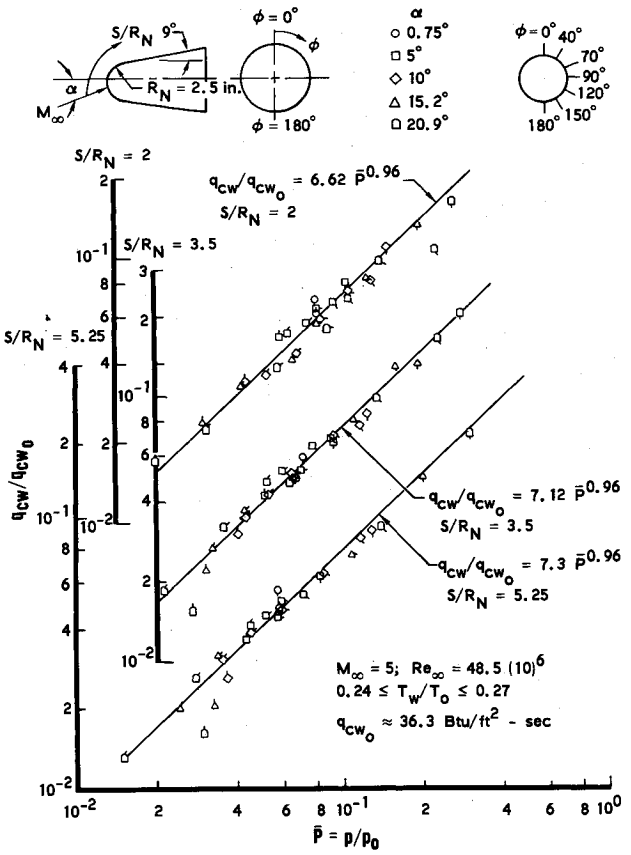

Fig. 10 Correlation of the turbulent heat-transfer data at stations $S/R_N = 2$, 3.5 and 5.25.

rather than edge conditions to define the local heat-transfer rate. Specifically, the McCuen et al., and Walker relation substantially overpredict the peak heating for these test conditions and, in general, overpredict the rates on the conical surface as well. The formulation of DeJarnette and Tai yields results for these test conditions which are, in general, a few percent higher than the respective rates calculated using the Vaglio-Laurin relation.

4) The turbulent heat-transfer correlation for blunt cones at angle of attack which was previously demonstrated in Ref. 3 was shown to be applicable.

5) Numerical calculations of the surface pressure agree with the measured distributions except in regions where viscous-inviscid interactions become important.

References

[1] Widhopf, G. F., "Turbulent Heat Transfer Measurements on a Blunt Cone at Angle of Attack," TR-0059(S6816-66)-1, Feb. 1971, The Aerospace Corp., San Bernardino, Calif.; also *AIAA Journal*, Vol. 9, No. 8, Aug. 1971, pp. 1574–1580.

[2] Zakkay, V. and Sakell, L., "Laminar, Transition and Turbulent Heat Transfer to the Leeward Side of Axially Symmetric Bodies," New York Univ., N.Y., to be published.

[3] Widhopf, G. F., "Heat Transfer Correlations for Blunt Cones at Angle of Attack," TR-0172(S2816-63)-1, July 1971, The Aerospace Corp., San Bernardino, Calif.; also *Journal of Spacecraft and Rockets*, Vol. 8, No. 9, Sept. 1971, pp. 1002–1004.

[4] Geineder, F., Schlesinger, M. I., Baum, G., and Cornett, R., "The U.S. Naval Ordnance Laboratory Hypersonic Tunnel," NOLTR 67-27, April 1967, U.S. Naval Ordnance Lab., White Oak, Md.

[5] Baltakis, F. P., "Performance Capability of the NOL Hypersonic Tunnel," NOLTR 68-187, Oct. 1968, U.S. Naval Ordnance Lab., White Oak, Md.

[6] Widhopf, G. F., "Laminar, Transitional and Turbulent Heat Transfer Measurements on a Yawed Blunt Conical Nosetip," TR-0172 (S2816-60)-3, Aug. 1972, The Aerospace Corp., San Bernardino, Calif.

[7] Willis, J. W., "DARE II Data Acquisition and Recording Equipment for the Naval Ordnance Laboratory's Hypersonic Tunnel No. 8," NOLTR 63-281, 1964, U.S. Naval Ordnance Lab., White Oak, Md.

[8] Wilson, D. M. and Fisher, P. D., "Measurements of Hypersonic Turbulent Heat Transfer on Cooled Cones," Procedures of the **1966** *Heat Transfer and Fluid Mechanics Institute*, Stanford University Press, Stanford, Calif., 1966.

[9] Nagel, A. L., Fitzsimmons, H. D., and Doyle, L. B., "Analysis of Hypersonic Pressure and Heat Transfer Tests on Delta Wings with Laminar and Turbulent Boundary Layers," NASA CR-535, Aug. 1966, The Boeing Co., Seattle, Wash.

[10] Hall, R., "The Turbulent Heat Transfer on the Spherical Portion of a Blunted Cone at High Angles of Attack at $M_\infty = 5$," NOLTR 1972, U.S. Naval Ordnance Lab., White Oak, Md., in publication.

[11] Risher, D. B., "Multiple Pressure Transducer Banks and Their Application," NOLTR 67-148, 1967, U.S. Naval Ordnance Lab., White Oak, Md.

[12] Abbett, M. J. and Fort, R., "Three-Dimensional Inviscid Flow about Supersonic Blunt Cones at Angles of Attack, III: Coupled Subsonic and Supersonic Programs for Inviscid Three-Dimensional Flow," Sandia Labs. SC-CR-68-3728, Sept. 1968, General Applied Science Labs., Westbury, N. Y.

[13] Fay, J. A. and Riddell, F. R., "Theory of Stagnation Point Heat Transfer in Dissociated Air," *Journal of the Aeronautical Sciences*, Vol. 25, No. 2, Feb. 1958, pp. 73–85.

[14] Mateer, G. G., "Effects of Wall Cooling and Angle of Attack on Boundary Layer Transition on Sharp Cones at M = 7.4," NASA Ames Research Center, Moffett Field, Calif., presented at the Boundary Layer Transition Specialists Workshop held at The Aerospace Corp., San Bernardino, Calif., Nov. 1971.

[15] Mateer, G. G. and Larson, H. K., "Unusual Boundary Layer Transition Results on Cones in Hypersonic Flow," *AIAA Journal*, Vol. 7, No. 4, April 1969, pp. 660–664.

[16] Otis, J. H., Jr., et al., "Strategic Reentry Technology Program (STREET-A), Final Report, Vol. II," AVSD-0210-70-RR, Vol., II, Nov. 1970, Avco Systems Div., Wilmington, Mass.

[17] Vaglio-Laurin, R., "Laminar Heat Transfer on Three-Dimensional Blunt Nosed Bodies in Hypersonic Flow," *ARS Journal*, Vol. 29, No. 2, Feb. 1959, pp. 123–129.

[18] Chen, K. K. and Tyson, N. A., "Extension of Emmons' Spot Theory to Flows on Blunt Bodies," *AIAA Journal*, Vol. 9, No. 5, May 1971, pp. 821–825.

[19] Vaglio-Laurin, R., "Turbulent Heat Transfer on Blunt-Nosed Bodies in Two-Dimensional and General Three-Dimensional Hypersonic Flow," *Journal of the Aerospace Sciences*, Vol. 27, No. 1, Jan. 1960, pp. 27–36.

[20] McCuen, P. A., Schaefer, J. W., Lundberg, R. E., and Kendall, R. M., "A Study of Solid-Propellant Rocket Motor Exposed Material Behavior," Final Rept. 149, Feb. 1965. Vidya Div., Itek Corp., Mountain View, Calif.

[21] Walker, G. K., "A Particular Solution to the Turbulent Boundary Layer Equation," *Journal of the Aerospace Sciences*, Vol. 27, No. 9, Sept. 1960, pp. 715–716.

[22] De Jarnette, F. R. and Tai, T. C., "A Method for Calculating Laminar and Turbulent Convective Heat Transfer Over Bodies at an Angle of Attack," NASA CR-101678, March 1969, Virginia Polytechnic Inst., Blacksburg, Va.

[23] Cebeci, T. and Smith, A. M. O., "A Finite Difference Method for Calculating Compressible Laminar and Turbulent Boundary Layers," *Journal of Basic Engineering*, Vol. 92, No. 3, Sept. 1970, pp. 523–535.

[24] Beckwith, I. E. and Gallagher, J. J., "Heat Transfer and Recovery Temperatures on a Sphere with Laminar, Transitional, and Turbulent Boundary Layers at Mach Numbers of 2. 00 and 4. 15," TN 4125, 1957, NACA.

[25] Stetson, K. F., "Boundary-Layer Transition of Blunt Bodies with Highly Cooled Boundary Layers," *Journal of the Aerospace Sciences*, Vol. 27, No. 2, Feb. 1960, pp. 81–91.

[26] Bandettini, A. and Isler, W. E., "Boundary-Layer Transition Measurements on Hemispheres of Various Surface Roughness in a Wind Tunnel at Mach Numbers from 2.48 to 3.55," Memo 12-25-58A, 1959, NASA.